Cell Metabolism
Article

Adipose Vascular Endothelial Growth Factor Regulates Metabolic Homeostasis through Angiogenesis

Hoon-Ki Sung,[1] Kyung-Oh Doh,[2] Joe Eun Son,[1] Jin Gyoon Park,[1] Yunui Bae,[2] Soojeong Choi,[1] Seana Mary Lunney Nelson,[1,7] Rebecca Cowling,[1] Kristina Nagy,[1] Iacovos P. Michael,[1] Gou Young Koh,[3] S. Lee Adamson,[1,4,5] Tony Pawson,[1,6] and Andras Nagy[1,5,7,*]

[1]Samuel Lunenfeld Research Institute, Mount Sinai Hospital, Toronto, ON M5T 3H7, Canada
[2]Department of Physiology, College of Medicine and Aging-Associated Vascular Disease Research Center, Yeungnam University, Daegu 705-717, Korea
[3]National Research Laboratory of Vascular Biology and Graduate School of Medical Science and Engineering, Korea Advanced Institute of Science and Technology (KAIST), Daejeon 305-701, Korea
[4]Department of Physiology
[5]Department of Obstetrics and Gynecology
[6]Department of Molecular Genetics
[7]Institute of Medical Science
University of Toronto, Toronto, ON M5S 1A8, Canada
*Correspondence: nagy@lunenfeld.ca
http://dx.doi.org/10.1016/j.cmet.2012.12.010

SUMMARY

Vascular endothelial growth factor A (VEGF) is highly expressed in adipose tissue. Its role, however, has not been fully elucidated. Here, we reveal the metabolic role of adipose-VEGF by studying mice with deletion ($VEGF^{Ad\Delta}$) or doxycycline-inducible overexpression of a VEGF transgene ($VEGF^{AdTg}$) in the adipose tissue. $VEGF^{Ad\Delta}$ mice have reduced adipose vascular density and show adipose hypoxia, apoptosis, inflammation, and metabolic defects on a high-fat diet. In contrast, induction of VEGF expression in $VEGF^{AdTg}$ mice leads to increased adipose vasculature and reduced hypoxia. The latter changes are sufficient to counteract an established compromising effect of high-fat diet on the metabolism, indicating that metabolic misbalance is reversible by adipose vessel density increase. Our data clearly show the essential role of VEGF signaling for adequate adipose function. Besides revealing insights into the molecular mechanisms of obesity-related metabolic diseases, this study points to the therapeutic potential of increased adipose angiogenesis.

INTRODUCTION

Obesity, defined as an excess of whole-body adipose tissue, has become a global health problem and a leading cause of several chronic illnesses, including type 2 diabetes (WHO, 2010; Yach et al., 2006). There is increasing evidence that adipose tissue does not simply store energy but is also an essential endocrine organ, producing hormones and secreting growth factors and chemokines (Waki and Tontonoz, 2007), commonly termed adipokines. These molecules are crucial for both local and systemic communication between adipose and other tissues.

The connection between obesity and metabolic diseases is well established, and increasing efforts are taken to unveil the mechanisms underlying this association. Obesity is accompanied by major changes in the properties of the adipose tissue, including elevated expression of proinflammatory markers, such as CRP, IL-6, TNFα, MCP-1, and MIF (Hotamisligil, 2006; Wellen and Hotamisligil, 2005). These inflammatory factors are major contributors to the metabolic disease phenotype (Weisberg et al., 2003; Xu et al., 2003). On the other hand, adiponectin, a hormone produced exclusively by adipose tissue, plays a positive modulatory role in glucose regulation and suppression of the metabolic syndrome and type 2 diabetes (Yamauchi et al., 2001, 2002).

Adipose tissue is characterized by its ability for lifelong growth and almost unlimited expansion. As in other tissues, fat expansion requires concomitant neovascularization to enable delivery of oxygen and nutrients (Cao, 2007; Christiaens and Lijnen, 2010; Hausman and Richardson, 2004; Lijnen, 2008). To promote neovascularization during its expansion, adipose tissue expresses various angiogenic growth factors, such as vascular endothelial growth factor (VEGF), fibroblast growth factor (FGF), placental growth factor (PlGF), and leptin (Cao, 2007; Lijnen et al., 2006; Miyazawa-Hoshimoto et al., 2003).

Similar to tumor neovascularization (Kerbel, 2008), the critical role of adipose vasculature in tissue growth has generated much interest. Efforts have been made to utilize inhibition of angiogenesis as a potential therapeutic approach for the treatment of obesity and/or diabetes. Indeed, a number of systemically applied angiogenesis inhibitors have shown preliminary efficacy and promise in preclinical models of obesity and metabolic dysfunction (Bråkenhielm et al., 2004; Cao, 2010; Liu et al., 2010; Rupnick et al., 2002). Several hypotheses have been proposed to explain the inflammatory response of adipose tissue to pathologic expansion, including oxidative stress (Houstis

et al., 2006), endoplasmic reticulum stress (Gregor and Hotamisligil, 2007; Ozcan et al., 2004), and hypoxia (Hosogai et al., 2007; Trayhurn et al., 2008). Although these possible mechanisms could be interrelated, hypoxia is likely to play key causal roles in adipocyte dysfunction and the development of insulin resistance (Chi et al., 2006; Goossens et al., 2011; Hosogai et al., 2007; Pasarica et al., 2009, 2010; Wood et al., 2009; Trayhurn et al., 2008; Yin et al., 2009) by inducing inflammation, which in turn leads to massive changes in adipokine profiles and ectopic lipid deposition in insulin sensitive organs. Hypoxia in the adipose tissues of *ob/ob* and diet-induced obese (DIO) mice has been linked to inadequate angiogenesis (Hosogai et al., 2007; Yin et al., 2009), which could point to insufficient adipose VEGF signaling as the initiating element of a cascade of events that leads to metabolic diseases.

To shed further light on these events, we developed two kinds of genetically modified mice in which adipose-specific blood vessel density is modulated: adipose-specific deletion of VEGF ($VEGF^{Ad\Delta}$), and doxycycline-inducible overexpression of VEGF ($VEGF^{AdTg}$). Importantly, the specificity of deletion and transgene overexpression is identical. We show that mice selectively deficient for adipose VEGF develop an abnormally sparse adipose vascular network. The decreased vessel density has dramatic negative effects on the metabolic phenotype of these animals. Conversely, adipose-specific expression of VEGF not only protects mice from development of metabolic abnormalities (Hagberg et al., 2010; Liu et al., 2010) but also improves already compromised metabolic functions brought on by a high-fat diet. These findings strongly support our hypothesis that insufficient adipose VEGF signaling initiates a cascade of events that ends with metabolic disease. Furthermore, they show that restoring adequate vessel density in metabolically challenged obese individuals reverts the disease. The latter opens up a new avenue for novel therapeutic approaches.

RESULTS

Adipose-Specific Ablation of VEGF Results in Reduced Vascular Density and Growth of Adipose Tissue

Adipocytes and resident macrophages are the major sources of VEGF in adipose tissues (Cho et al., 2007; Mick et al., 2002; Zhang et al., 1997). We knocked out VEGF specifically in these two cell types to determine its effect on adipose blood vessel development. We then crossed mice bearing a Cre recombinase-conditional VEGF allele ($VEGF^{loxP}$) (Gerber et al., 1999) with those harboring an aP2-Cre recombinase transgene (see Figure S1A online). The latter is very well characterized and known to restrict expression to adipocytes and macrophages (He et al., 2003). Mice with the genotypes marked as ''control'' in Figure S1A were phenotypically indistinguishable from wild-type mice (data not shown).

Adipose tissue-specific VEGF knockout mice ($aP2\text{-}Cre^{(+)}$; $VEGF^{(loxP,loxP)}$, hereafter referred to as $VEGF^{Ad\Delta}$) were born at the expected Mendelian ratio, were viable and fertile, and showed no gross abnormalities (data not shown). Only trace amounts of mRNA and VEGF protein were detected in their white (WAT) and brown (BAT) adipose tissues by quantitative PCR and western blot, respectively (Figures 1A and 1B). In contrast, the VEGF mRNA levels in other tissues, such as muscle and liver, and the serum level of VEGF were similar to those of controls (Figures 1A and 1C), confirming the adipose-specific loss of VEGF. The gross appearance of WAT from $VEGF^{Ad\Delta}$ mice was pale compared to that of the controls (Figure 1D, panel Gross), suggesting reduced blood perfusion. When blood vessels were visualized by whole-mount immunostaining using a PECAM-1 antibody, it was evident that the vascular densities of both WAT and BAT in $VEGF^{Ad\Delta}$ mice were significantly lower than in the control (Figures 1D [panels PECAM-1], Figures 1E and 1F).

To rule out the possibility of an autocrine effect of VEGF modulation on adipocyte function, we studied two gene-targeted mouse lines with lacZ knocked into the loci for either the Flk1 (Ema et al., 2006) or the Flt1 (Fong et al., 1995) VEGF receptors. X-gal-stained WAT and BAT from these mice revealed that the receptors were expressed by endothelial cells (Figure S1B, yellow arrowheads), but not by white or brown adipocytes (Figure S1B, red arrows). We therefore conclude that the effect of VEGF on adipose function is manifested in a paracrine manner through blood vessels.

Given the critical importance of adequate angiogenesis for tissue growth, we inferred that reduced adipose vascularization in $VEGF^{Ad\Delta}$ mice may hinder fat tissue expansion and, consequently, body weight gain. Consistent with this expectation, the juvenile body weight of these animals was slightly lower than that of controls (Figure 1G). Magnetic resonance-assisted measurements of body composition revealed a significant reduction in their fat mass, while their lean mass remained similar to controls (Figure 1H). Subsequent weight measurements of fat tissues harvested from these mice showed that the reduction in fat weight was more prominent in perigonadal (PGF) than in subcutaneous fat (SCF) (Figure 1I). Since Cre-recombinase activity level is identical in these two tissues (data not shown), these findings indicate a higher sensitivity of perigonadal fat to adipose VEGF deletion than that of subcutaneous fat. The adipocyte size in WAT and weight of the BAT in the $VEGF^{Ad\Delta}$ mice was not significantly different from those of controls (data not shown). Furthermore, histological examination of the liver and skeletal muscle did not reveal any difference between experimental groups (data not shown). In summary, the above studies showed that adipose VEGF ablation decreased fat tissue vascularity with a concurrent fat mass reduction in WAT.

Altered Adipokine Expression in the WAT of $VEGF^{Ad\Delta}$ Mice

Next, we investigated the changes in metabolic parameters and the gene expression level on a panel of thermo- and lipogenic genes in 12- to 16-week-old $VEGF^{Ad\Delta}$ animals. The reduced vascularization (Figure 1D, middle panel, and Figure 1E) was accompanied by a significantly reduced population of endothelial cells in the WAT, indicated by a decreased level of VEGFR-2 in this tissue (*Flk1*; Figure 1J). We found no differences in food consumption (Figure S1C), serum triglyceride (TG) (data not shown), or fasting glucose levels, or in intraperitoneal glucose tolerance tests (Figure S1D). Furthermore, similar serum insulin levels (data not shown) indicated a normal glucose homeostasis in $VEGF^{Ad\Delta}$ animals. While mRNA levels of most adipogenic or adipose secreted factors were unchanged (Figure S1E), the expression of adiponectin, an antidiabetic adipokine, was significantly reduced (Figure 1K), and expression of TNF-α,

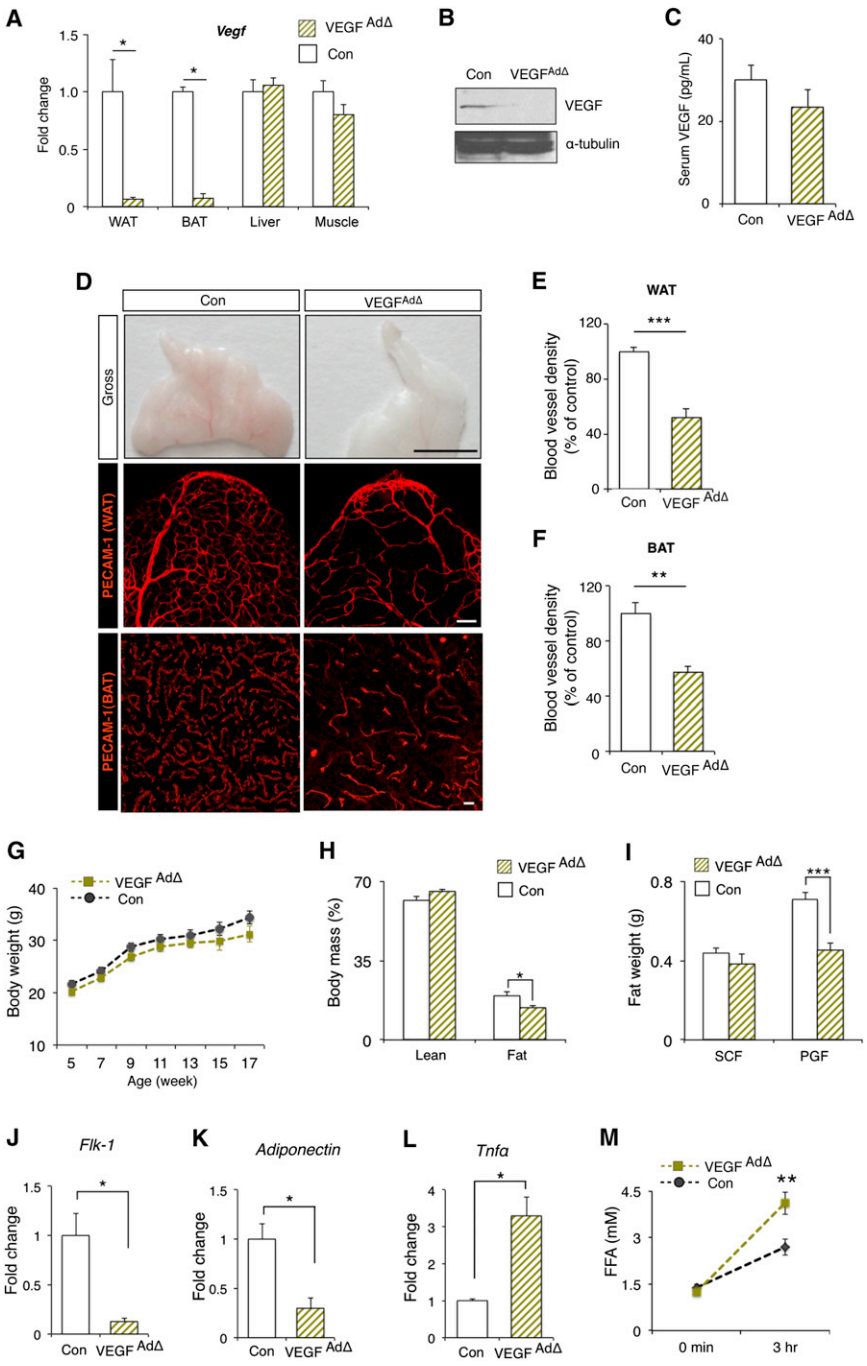

Figure 1. Phenotypic Consequences of VEGF Ablation in the Adipose Tissues of Animals Maintained on Standard Chow

(A) Quantitative PCR analysis for VEGF gene expression in white and brown adipose tissue (WAT and BAT, respectively), liver, and skeletal muscle (n = 4 for both groups).

(B) Western blotting analysis for tissue VEGF protein in WAT.

(C) Serum VEGF concentration determined by ELISA (n = 6 for control, n = 10 for $VEGF^{Ad\Delta}$).

(D) Upper panel, gross appearance of WAT. Middle and lower panels, confocal microscopic image of whole-mount WAT and cryosectioned BAT immunostained with PECAM-1 antibody to show vessel density.

(E and F) Quantification of vessel densities of both WAT (E) and BAT (F) by intensity of the immunofluorescent signal (WAT, n = 5 for control, n = 7 for $VEGF^{Ad\Delta}$; BAT, n = 4 for both).

(G) Body weight changes with age (n = 10–15 for control, n = 6–16 for $VEGF^{Ad\Delta}$).

(H) Magnetic resonance-assisted determination of percent fat and lean mass (n = 6 for both groups).

(I–L) (I) Fat weight (n = 5 for both groups). qPCR analysis of *Flk-1* (J), *Adiponectin* (K), and *Tnfα* (L) expression in WAT (n = 3–4 for both groups).

(M) Serum-free fatty acid level at fasting and 3 hr after oil gavage (n = 7 for both groups).

All data are presented as mean ± SEM. *p < 0.05, **p < 0.01, ***p < 0.005. Scale bars, 0.5 cm in (D) upper panel and 100 μm in all microscopic images.

a proinflammatory cytokine, was significantly elevated (Figures 1L). Fasting free fatty acid (FFA) in the serum was the same as in the control. Oral lipid challenge, however, dramatically increased FFA in $VEGF^{Ad\Delta}$ animals, indicating a defective lipid handling capability (Figure 1M).

Interestingly, some of the thermo- and lipogenic gene expression levels were lower in the BAT of the $VEGF^{Ad\Delta}$ animals (Figure S1F), but this decrease did not affect the energy expenditure and ambulatory activity (Figures S1G and S1H) of the animals.

$VEGF^{Ad\Delta}$ Mice Develop Metabolic Defects and Insulin Resistance on a High-Fat Diet

Although $VEGF^{Ad\Delta}$ animals were slightly leaner than the controls, they developed a mild metabolic impairment when kept on standard chow (SC). This finding prompted us to challenge these animals with a high-fat diet (HFD, 60% of calories from fat), expecting an accelerated development of their metabolic disease. We based this expectation on the observation of increased adipose VEGF expression on HFD both in normal (Figure S2A) and in *ob/ob* mice (Halberg et al., 2009). From 12 weeks of age, the experimental and control mice were kept on HFD, and their body weights were monitored. During the first 3 weeks, the $VEGF^{Ad\Delta}$ animals showed only a slightly lower weight gain than controls; however, over time, a wider difference (Figure 2A) and less fat mass development became apparent in these animals (Figure 2B), while the size of the adipocytes remained comparable (Figure S2B). Freshly harvested WAT from $VEGF^{Ad\Delta}$ animals were darker than that of the controls (Figure 2C, panel Gross), and histological examination revealed high levels of inflammatory cell infiltration into the VEGF-deficient tissues (Figure 2C, panel WAT [H&E]).

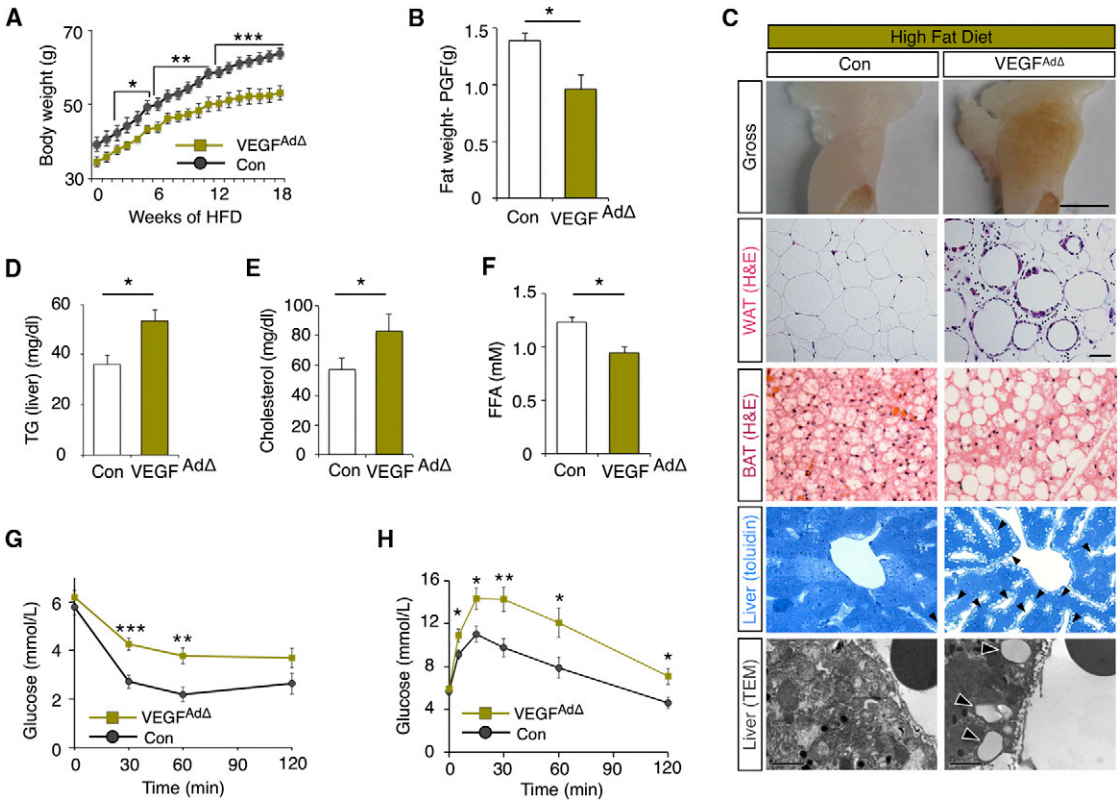

Figure 2. Metabolic Consequences of Ablation of VEGF in Adipose Tissue in Animals Kept on High-Fat Diet

(A) Body weight changes of experimental animals during HFD feeding (n = 9 for control, n = 6 for VEGF$^{Ad\Delta}$).

(B) WAT (Perigonadal fat, PGF) weight measurement after 18 weeks of HFD feeding (n = 6 for both groups).

(C) Histopathological changes in VEGF$^{Ad\Delta}$ mice after HFD. (Gross), gross appearance of WAT; WAT (H&E), hematoxylin and eosin staining of WAT; BAT (H&E), hematoxylin and eosin staining of brown adipose tissue; Liver (toluidine), toluidine blue staining of semithin sectioned liver tissue. Black arrowheads indicate localization of cytoplasmic vacuoles in hepatocytes in VEGF$^{Ad\Delta}$ mice. Liver (TEM), transmission electron microscopic examination of liver of HFD-fed animals. Arrowheads indicate cytoplasmic vacuolation in hepatocytes.

(D–F) (D) Liver triglyceride (TG), (E) serum measurement of fasting cholesterol, and (F) serum-free fatty acid concentrations (n = 5–9 for both groups).

(G) Insulin (ITT) and (H) glucose tolerance test (IPGTT) after HFD (n = 13 for control, n = 11 for VEGF$^{Ad\Delta}$).

All data are presented as mean ± SEM. *p < 0.05, **p < 0.01, ***p < 0.005. Scale bars, 0.5 cm in (C) upper panel and 100 μm in all microscopic images.

Interestingly, many brown adipocytes in VEGF$^{Ad\Delta}$ mice resembled a white adipocyte-like unilocular, rather than a typical multilocular, morphology (Figure 2C, panel BAT [H&E]). In the livers of VEGF$^{Ad\Delta}$ animals, numerous cytoplasmic vacuoles were localized around the portal veins (data not shown) and were present in the hepatocytes close to the hepatic sinusoidal endothelium (Figure 2C, panel Liver [toluidine] and panel Liver [TEM]). The electron density of these vacuoles was comparable to that of the lipid droplets in adipocytes (data not shown), which was consistent with the increased liver triglyceride level of the VEGF$^{Ad\Delta}$ animals (Figure 2D). Thus the pathological manifestation of a HFD challenge was presented in both white and brown adipose tissue, as well as in the hepatocytes of the VEGF$^{Ad\Delta}$ mice, implying that these animals may have global defects in their metabolic homeostasis.

Although there were no differences in fasting blood glucose levels and in expression of *Fabp4* and *VEGF* in liver and muscle (Figures S2C and S2D) after 18 weeks on HFD, the VEGF$^{Ad\Delta}$ animals showed significantly elevated total cholesterol (Figure 2E) and decreased fasting level of FFA levels in the serum (Figure 2F). More importantly, the VEGF$^{Ad\Delta}$ animals developed severe insulin resistance (Figure 2G) and glucose intolerance (Figure 2H).

VEGF$^{Ad\Delta}$ Animals on a High-Fat Diet Show Increased Macrophage Infiltration, Adipocyte Apoptosis, and Inflammation of White Adipose Tissues

Immunohistochemical staining with an F4/80 antibody proved the macrophage origin of the inflammatory cells infiltrating the adipose tissue in HFD-fed VEGF$^{Ad\Delta}$ animals (Figures 3A and 3B). The macrophages were highly concentrated (Figures 3C and 3E) in areas with low or no perilipin signal (Figures 3C and 3D), possibly marking the location of apoptotic adipocytes where macrophages are performing their scavenging function (Cinti et al., 2005; Strissel et al., 2007). Elevated numbers of active caspase-3-positive cells in VEGF$^{Ad\Delta}$ adipose tissue further supported this finding (Figures 3F and 3G).

Consistent with these observations, expression of inflammatory genes such as plasminogen activator inhibitor-1 (PAI-1), TNF-α, and macrophage chemotactic factor-1 (MCP-1) were

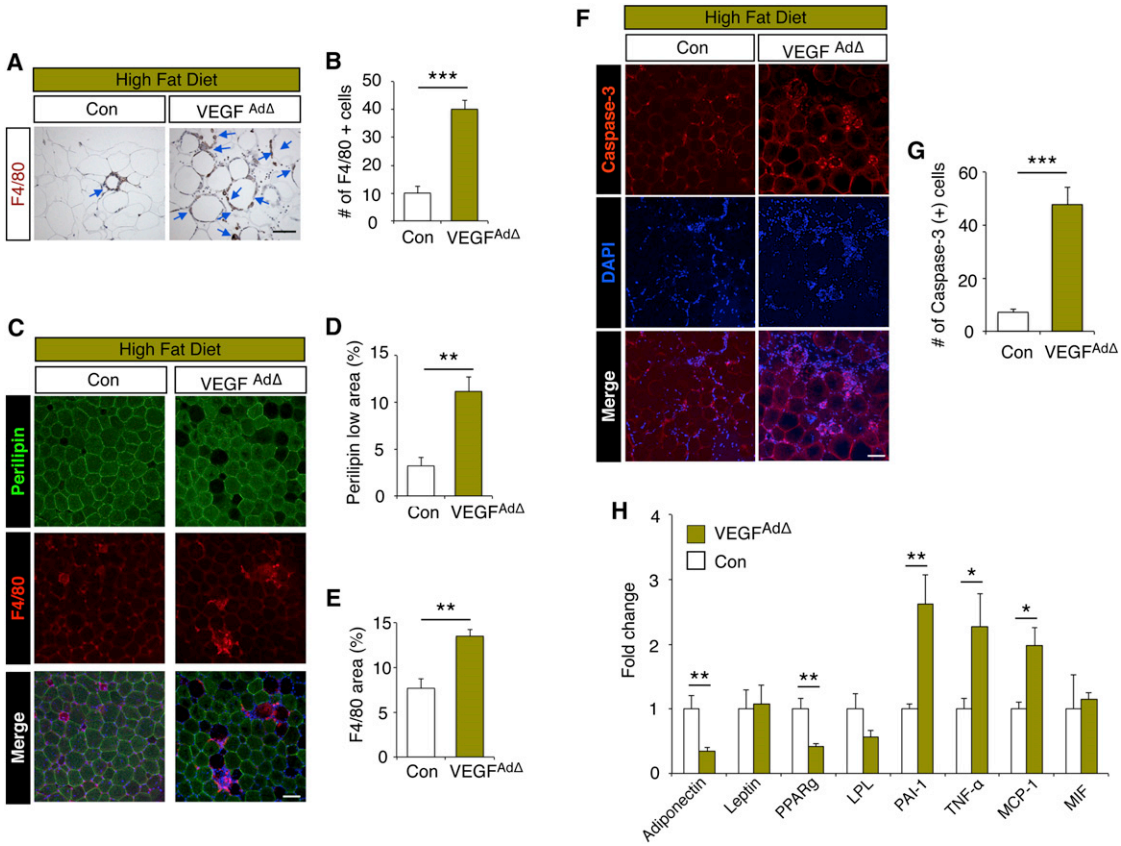

Figure 3. Properties of the Adipose Tissue of VEGF$^{Ad\Delta}$ Animals Kept on High-Fat Diet

(A) F4/80 immunohistochemistry detecting murine macrophage infiltration in WAT.

(B) Quantification of F4/80-positive cell numbers per field (n = 6 for both groups).

(C) Whole-mount WAT double stained with perilipin (adipocyte, green) and F4/80 (macrophage, red) antibodies.

(D and E) Percent area of (D) perilipin-low and (E) F4/80-positive regions (n = 6 for control, n = 5 for VEGF$^{Ad\Delta}$).

(F and G) (F) Immunofluorescent staining of whole-mount WAT with caspase-3 antibody and (G) its quantification (n = 6 for both groups).

(H) Gene expression analysis by qPCR (n = 5–9 per each group).

All data are presented as mean ± SEM. *p < 0.05, **p < 0.01, ***p < 0.005. Scale bars, 100 μm in all microscopic images.

also increased, while the expressions of adiponectin and PPARγ were significantly decreased (Figure 3H) in these mice. On the other hand, we did not find significant changes in apoptotic cell numbers and inflammatory cell infiltration in the BAT of VEGF$^{Ad\Delta}$ animals (data not shown) kept on HFD. Although we found decreased expression of some lipogenic genes in the BAT (Figure S3A), this did not result in any significant differences in energy expenditure or in total activity level (Figures S3B and S3C).

Since the adipose tissue in VEGF$^{Ad\Delta}$ mice was poorly vascularized, we investigated whether hypoxia could be part of the mechanism leading to adipocyte apoptosis. We detected significantly reduced vascular perfusion in the WAT of the VEGF$^{Ad\Delta}$ animals (Figures 4A and 4B). Consistent with this phenotype, the visualization of hypoxic areas by pimonidazole immunostaining of whole-mount adipose tissue revealed a 3-fold increase in hypoxic areas in VEGF$^{Ad\Delta}$ mice compared to controls (Figures 4C and 4D). We also compared the degree of hypoxia under different dietary conditions (Figure S4). Similar to findings in earlier studies (Hosogai et al., 2007), HFD resulted in increased adipose hypoxia compared to SC. The effect of HFD on adipose hypoxia was much more pronounced in VEGF$^{Ad\Delta}$ mice than in control animals (Figure S4).

Our results suggest that hypoxia is associated with adipocyte apoptosis and macrophage infiltration. This inflammation in the adipose tissue leads to abnormal production of adipokines and ectopic lipid depositions, to the known cause of glucose intolerance and insulin resistance (Virtue and Vidal-Puig, 2010; Weisberg et al., 2003; Xu et al., 2003).

Taken together, these data indicate that adipose VEGF is critical for maintaining the viability and metabolic/endocrine function of adipocytes through its role in regulating adequate vascularization and blood perfusion.

Generation and Characterization of Adipose-Specific Inducible VEGF164-Overexpressing Genetic Model

Our loss-of-function studies clearly showed the critical role of adipose VEGF and vessel density and suggested that hypoxia might be the cause for adipose dysfunction. We therefore expected that experimentally increased blood vessel density in

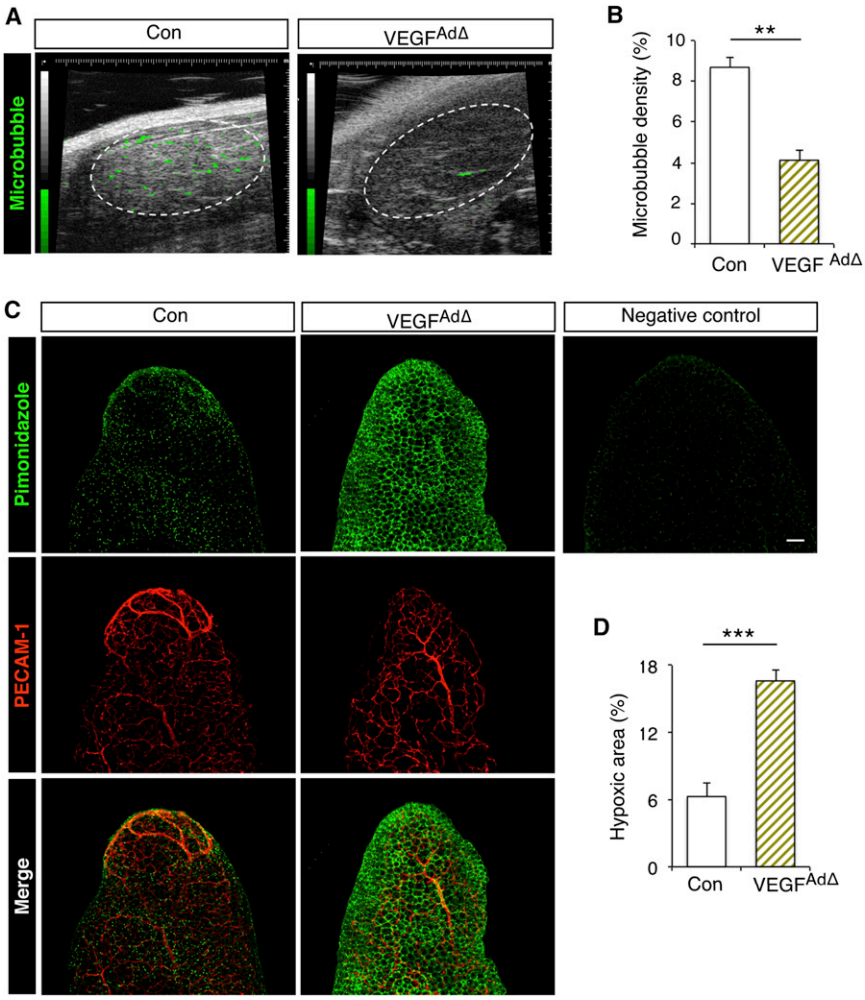

Figure 4. Consequences of Adipose Tissue Hypoperfusion in VEGF$^{Ad\Delta}$ Mice

Ultrasonic detection of WAT tissue perfusion using time course wash in of IV-injected microbubbles.

(A) Color-contrasted image of injected microbubble.

(B) Quantification of bubble (green signal inside dotted line of A) intensity (n = 6 for control, n = 5 for VEGF$^{Ad\Delta}$).

(C) Immunofluorescent staining of whole-mount WAT with pimonidazole and PECAM-1 antibodies to detect hypoxia and vessel density, respectively. Negative control, no primary antibody.

(D) Morphometric quantification of immunofluorescent signal in pimonidazole positive areas (n = 5 for control, n = 4 for VEGF$^{Ad\Delta}$).

All data are presented as mean ± SEM. **p < 0.01, ***p < 0.005. Scale bars, 100 μm in all microscopic images.

adipose tissue would have an opposite effect: reverting HFD-induced metabolic defects to a normal state. To this end, we crossed three well-characterized transgenic mouse lines: mice carrying a Cre recombinase conditional rtTA knockin into the Rosa26 locus (Belteki et al., 2005), a tet-O-VEGF164 (Akeson et al., 2003), and an aP2-Cre transgene (He et al., 2003). Triple transgenic animals (Figure 5A, designated VEGF^{AdTg}) were expected to overexpress VEGF164 exclusively in adipocytes and macrophages in a doxycycline (DOX)-inducible manner with the same specificity as the VEGF deletion in our loss-of-function model.

The appearance of the adipose tissue, blood vessel density, and adipocyte size in noninduced VEGF^{AdTg} mice was similar to that of controls, indicating that the transgene is silent in the absence of DOX (data not shown). To avoid possible negative effects (such as increased vascular permeability) of continuous VEGF164 induction (Ozawa et al., 2004), we applied a metronomically alternating DOX-on and DOX-off treatment regime consisting of a 4 day feeding period with SC followed by a 3 day feeding with doxycycline-containing SC (Standard/DOX diet regime, Figure 5B). After two cycles of this diet regime, freshly harvested WAT of DOX-treated VEGF^{AdTg} animals appeared more vascularized compared to control mice (single or double transgenic littermates; Figure 5C, upper panels). Whole-mount immunostaining with a PECAM-1 antibody revealed increased vascular density (Figures 5C, lower panels; Figure 5D) with numerous sprouting vascular tip cells, indicating that VEGF164 transgene induction resulted in active angiogenic processes in the adipose tissue of DOX-treated VEGF^{AdTg} animals (Figure 5C, lower panel, inset). There were no significant differences in body weight gain or food consumption between the two groups (Figure 5E and Figure S5A) during the observed period. Furthermore, we did not find any difference in random serum glucose levels (Figure 5F), intraperitoneal glucose tolerance, or insulin tolerance (Figures S5B and S5C).

We continued to characterize our adipose-specific inducible VEGF transgenic system in animals on HFD challenge. First we tested if we could recapitulate a recently published finding (Elias et al., 2012; Sun et al., 2012) that VEGF activation in adipose tissue at the time of HFD exposure protects animals from metabolic disease development. Similarly to the characterization on SC, here we applied the metronomic alternation of DOX-on and DOX-off treatment regime consisting of a 4 day feeding period with normal HFD followed by 3 day feeding with doxycycline containing high-fat chow (HFD/DOX diet regime) (Figure S6A). Four days after the start of the HFD feeding, we activated VEGF expression in the VEGF^{AdTg} animals using seven cycles of the HFD/DOX diet regime. The treatment resulted in a significant increase in VEGF164 expression both in WAT and in BAT, but not in the liver (Figure S6B). There was no difference in food intake, body weight gain, fat composition, fasting blood glucose levels, serum FFA, TG, total cholesterol, or glucose tolerance (data not shown) between the groups. However, while the control animals developed insulin resistance and hyperinsulinemia, the VEGF164-induced animals were protected from these (Figures S6C and S6D). Consistent with our

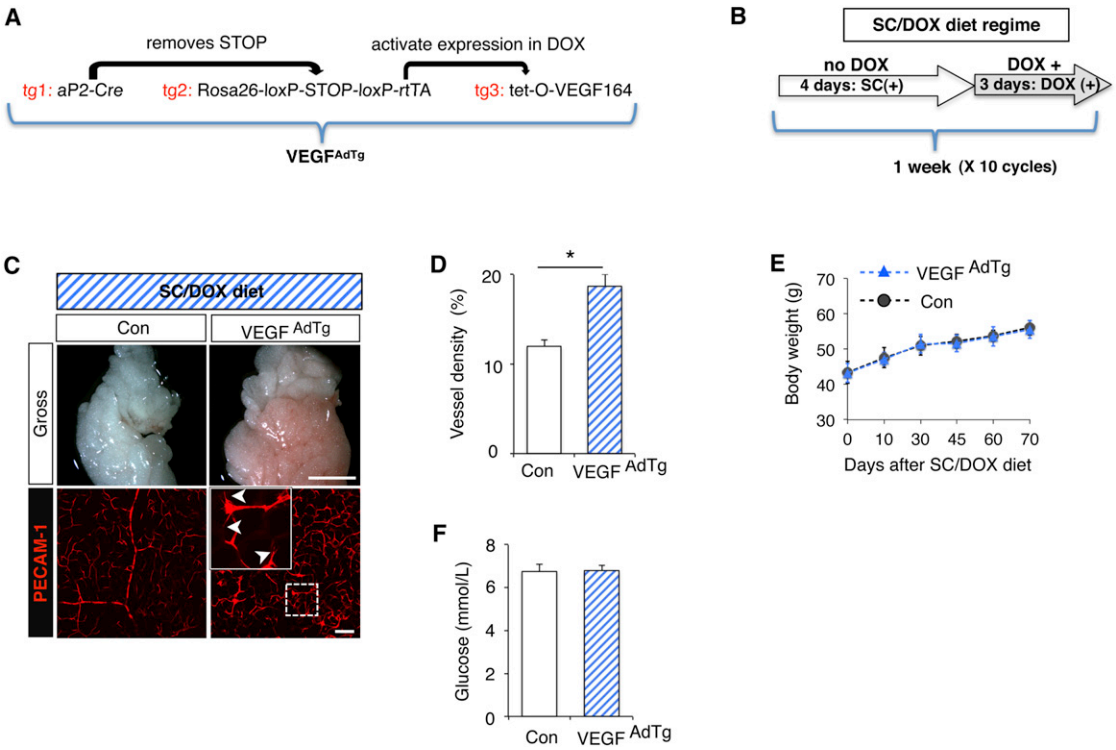

Figure 5. Generation and Basic Characteristics of Adipose-Specific Inducible VEGF164-Expressing Genetic Mouse Model

(A) Generation of adipose-specific and doxycycline-inducible VEGF164 triple transgenic mice (VEGF^{AdTg}).

(B) Schematics of metronomic induction of VEGF164 with standard chow (SC) and doxycycline-containing chow (DOX) (Standard/DOX diet regime).

(C) Gross appearance (upper panel) and PECAM-1 staining (lower panel) of WAT after two cycles of SC/DOX diet regime.

(D) Body weight changes during ten cycles of SC/DOX diet regime (n = 8 for control, n = 6 for VEGF^{AdTg}).

(E) Fasting blood glucose level after ten cycles of Standard/DOX diet regime (n = 7 for both groups).

All data are presented as mean ± SEM. *p < 0.05. Scale bars, 0.5 cm in (C) upper panel and 100 μm in all microscopic images.

loss-of-function analysis, WATs from control mice showed increased inflammatory cell infiltration (Figure S6E, panel WAT, arrowheads). We also observed elevated lipid deposition in the BAT and liver (Figure S6E, panel BAT [H&E] and Liver [H&E]) and enlarged islet cell mass (Figure S6E, panel Pan [H&E]). Therefore, we concluded that when VEGF induction and HFD challenge were applied simultaneously, aP2-specific induction VEGF protects animals from HFD-induced metabolic defect and insulin resistance. We then attempted to identify the mechanism underlying the protective effect of VEGF in these mice and investigated whether it was mediated through the modulation of adipose vessel density and hypoxia. Whole-mount PECAM-1 staining showed an increased vascular network in the adipose tissue of the DOX-induced VEGF^{AdTg} animals (Figure S6F, panel PECAM-1), resulting in increased tissue perfusion compared to that of the controls (Figure S6F, panel Microbubble). Consistent with these observations, hypoxia was significantly decreased in the WAT of VEGF^{AdTg} mice (Figure S6F, panel Pimonidazole), which was accompanied by higher expression of adiponectin and PPARγ and lower expression inflammatory cytokine TNF-α (Figure S6G). The level of circulating adiponectin was also significantly higher in VEGF^{AdTg} animals (Figure S6H). Decreased hypoxia was associated with a lower level of caspase-3 expression (Figure S6G), reduced caspase-3-positive cell number (Figures S6I and S6J), and inflammatory cell infiltration in the adipose tissue of VEGF^{AdTg} mice compared with controls (Figure S6E, panel WAT). Although adipocyte size was reduced, we did not detect significant differences in blood vessel density or thermo- and lipogenic gene expression pattern in the BAT and energy expenditure of two groups (Figures S6K–S6M), suggesting a moderate effect of VEGF164 on morphological and functional changes in BAT.

Transgenic Expression of VEGF164 Reverts High-Fat-Diet-Induced Glucose Intolerance

We then asked if VEGF activation in the adipose could revert an already established metabolic disease induced by HFD. First we challenged the VEGF^{AdTg} (and controls animals) with HFD in the lack of doxycycline for 8 weeks. Then we applied four cycles of metronomic treatment of HFD/DOX diet regime (Figure 6A). The animal's body weight and glucose tolerance were monitored at Start and Term as well as weekly during the study (Figures 6B and 6C). After 8 weeks of HFD feeding (at Start), glucose clearance was delayed in both groups—reflected by high AUC values—indicating their glucose intolerant status (Figure 6C, at Start). After four metronomic cycles of the HFD/DOX diet (at Term), we found a surprising reversal effect on glucose intolerance accompanied with dramatic reduction in body weight and

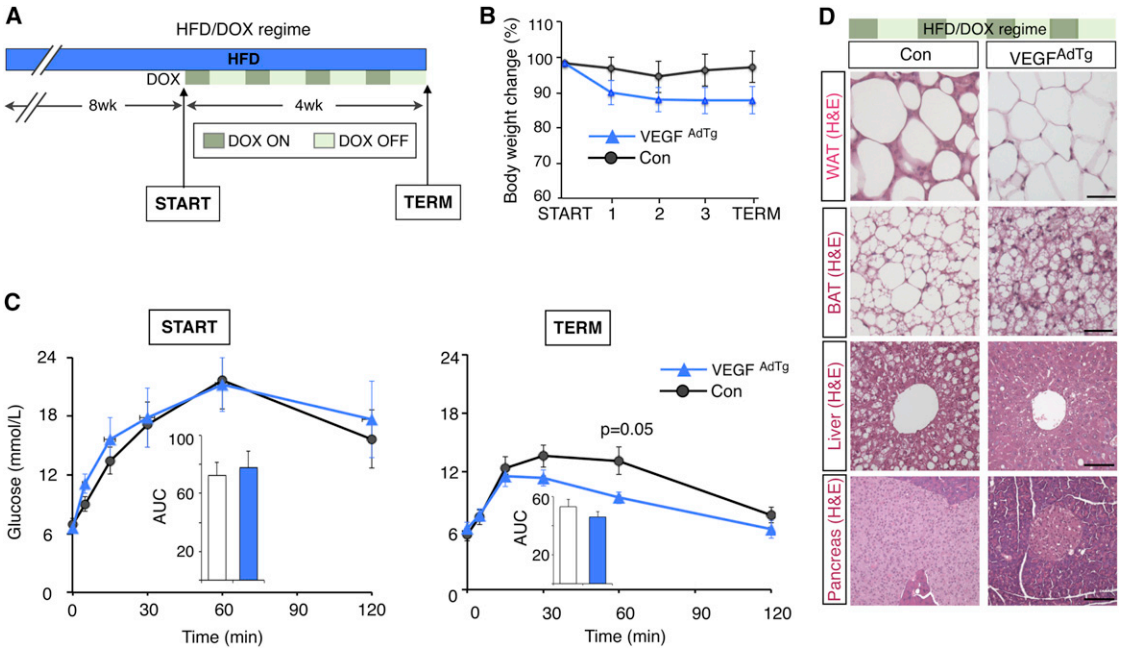

Figure 6. Metronomic Induction of VEGF164 Expression Improves Glucose Tolerance in Diet-Induced Obese Mice

(A) Schematics of metronomic induction of VEGF164 with high-fat diet (HFD) and doxycycline-containing HFD (HFD/DOX regime). HFD was given for 8 weeks followed by metronomic 3 days of DOX ON and 4 days of DOX OFF cycle as indicated in control and VEGF^{AdTg} mice.

(B) Body weight was monitored during the HFD/DOX treatment (represented as a percent of initial body weight) (n = 6–8 per each group).

(C) Left panel, intraperitoneal glucose tolerance test (IPGTT) at starting point of HFD/DOX regime (0 weeks) and its area under the curve (AUC). Right panel, IPGTT at 4 weeks after HFD/DOX metronomic treatment and its AUC (n = 6–8 per each group).

(D) Histopathological changes in control and VEGF^{AdTg} mice after 4 weeks of HFD/DOX regime. WAT (H&E), hematoxylin and eosin staining of WAT; BAT (H&E), hematoxylin and eosin staining of brown adipose tissue; Liver (H&E), hematoxylin and eosin staining of liver tissue; Pancreas (H&E), Liver (H&E), hematoxylin and eosin staining of pancreas. All data are presented as mean ± SEM. Scale bars, 25 μm in WAT and BAT, and 50 μm in liver and pancreas.

hepatic lipid deposition (Figures 6B and 6C [Term], Figure 6D). Besides the known, general glucose lowering effect of Dox treatment (Basaria et al., 2002; Garbitelli, 1987; Odeh and Oliven, 2000), our treated VEGF^{AdTg} animals showed improved glucose tolerance compared to the controls (Figure 6C, Term). This result is the first testament that a diagnosed metabolic disease is reversed by induced expression of adipose VEGF.

These data prompted us to challenge the 8 week HFD-exposed VEGF^{AdTg} mice with more aggressive DOX treatment and then a longer no-DOX time (Figure 7A). At Start we exposed animals to DOX for 2 weeks followed by 2 weeks of no DOX. At the start of the doxycycline treatment, the groups did not differ in their body weight, food consumption, or glucose tolerance (Figures 7B and 7C, Figures S7A and S7B). Similarly to the previous experiment, the high AUC indicated that glucose intolerance developed in both groups (Figure 7C, left panel). After feeding with HFD+DOX for 2 weeks, VEGF^{AdTg} mice showed a significant reduction in total body weight (Figure 7B), mostly due to the reduction of fat mass (Figure S7C). Most importantly, these mice showed significant improvement in glucose tolerance (Figure 7C, middle panel, and Figure S7D, middle panel DOX ENDs), while their circulating adiponectin was increased (Figure S7E). This improvement, however, was found to be VEGF induction dependent; the metabolic compromise rapidly re-established 2 weeks after the doxycycline treatment was stopped (Figure 7C, right panel, and Figure S7D, right panel).

We then evaluated whether increased vascular densities, and the resulting decrease in tissue hypoxia and inflammation, could be the possible mechanisms for the metabolic improvement in these animals. Indeed, we could observe reduced adipocyte size (Figure 7D, upper panels), increased vascular density (Figure 7D, middle panels), and reduced adipose hypoxia (Figure 7D, bottom panels) in VEGF^{AdTg} mice. Moreover, inflammatory CD11b and F4/80 double positive macrophage infiltration was also reduced in these animals (Figures 7E and 7F), which could further contribute to their metabolic improvement. There was no difference between the groups in food intake, rectal body temperature, fecal lipid content, energy expenditure, or serum lipid (FFA and TG) at Start and Term of the HFD/DOX regime (data not shown).

In summary, these data strongly suggested that adipose-specific VEGF164 expression could reverse metabolic anomalies. This reversal is mediated by suppression of hypoxia, inflammation, and apoptosis in the WAT. This leads to the restoration of normal secretion of adipokines and the inhibition of lipid accumulation in insulin-sensitive nonadipose tissues, and therefore improved metabolic homeostasis.

DISCUSSION

The development of obesity-related pathologic conditions, such as fatty liver, cardiovascular diseases, and type 2 diabetes, has

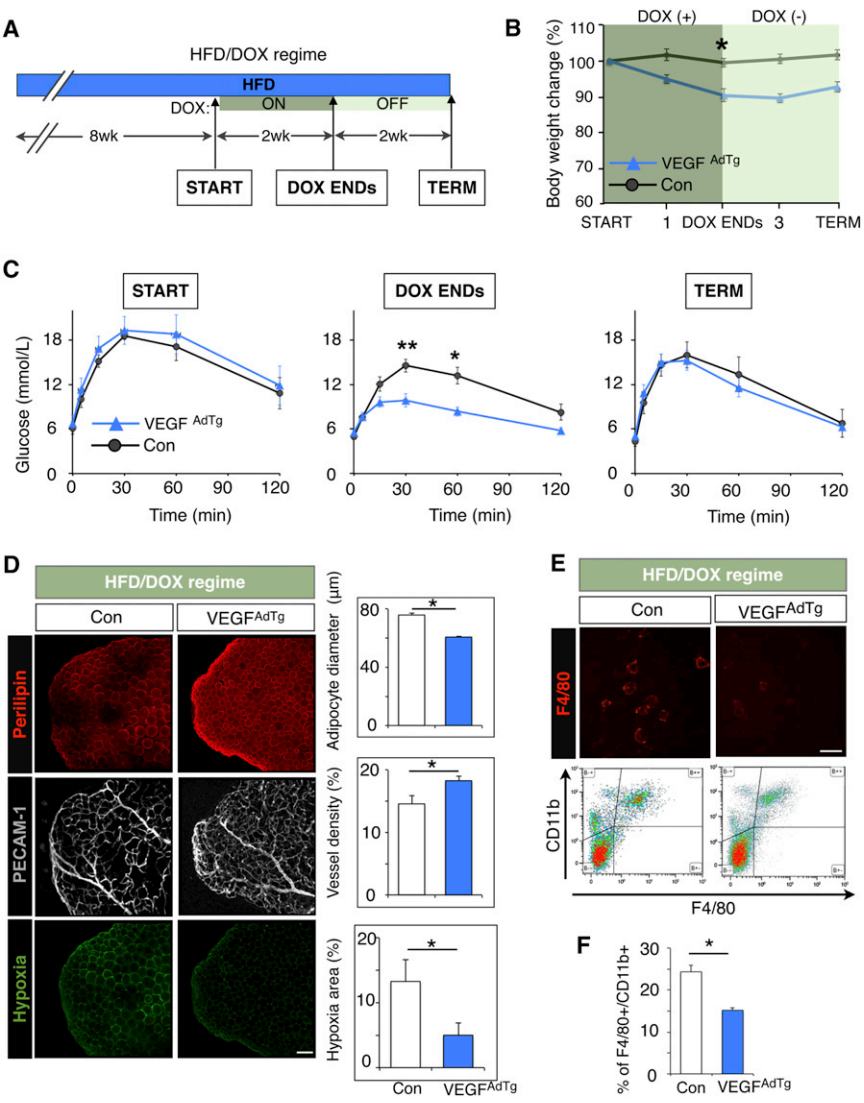

Figure 7. Induction of VEGF164 Reverts Glucose Intolerance in High-Fat-Diet-Induced Obese VEGF^{AdTg} Mice

(A) Schematics of VEGF164 induction and withdrawal. HFD was given for 8 weeks followed by metronomic 2 weeks of DOX ON (VEGF164 induction) and 2 weeks of DOX OFF (VEGF164 withdrawal) in control and VEGF^{AdTg} mice (n = 8 for control and n = 7 for VEGF^{AdTg} mice).

(B) Body weight change during the DOX treatment regime in control and VEGF^{AdTg} mice (n = 8 for control and n = 7 for VEGFAdTg mice; *p < 0.05).

(C) IPGTT in control and VEGF^{AdTg} mice at start (right panel, 0 weeks), 2 weeks after DOX (middle panel, 2wk DOX[+]) and 2 weeks after DOX withdrawal (right panel, 2wk DOX[−]) (n = 8 for control and n = 7 for VEGF^{AdTg} mice).

(D) Whole-mount immunostaining of adipose tissue from HFD-fed control and VEGF^{AdTg} mice. Top panel, perilipin staining and adipocyte diameter. Middle panel, PECAM-1 staining and its quantitation. Bottom panel, hypoxyprobe staining and its quantitation.

(E and F) Whole-mount immunostaining (E) and flow cytometry analysis (F) of macrophage in the adipose and its quantitation (n = 3–4 for both groups). All data are presented as mean ± SEM. *p < 0.05, **p < 0.01.

many underlying contributory elements, including nutritional status, lifestyle, and complex genetic factors. Mouse models have been used intensively to study the mechanisms behind the pathogenesis of these diseases (Hosogai et al., 2007; Yin et al., 2009). Hypoxia due to insufficient vascularization of the adipose tissue has been suggested as one important contributing factor (Hosogai et al., 2007). Recent human studies have confirmed that low vascular density in adipose tissues is directly associated with an abnormal metabolic profile (Pasarica et al., 2009, 2010). Obese patients often show decreased circulation and reduced perfusion rates in adipose tissues, which suggests that adipose hypoxia may play a role in the development of metabolic defects (Pasarica et al., 2009, 2010). These studies propose that adipose tissue hypoxia might be a link between obesity and its metabolic consequences. However, it is not clear whether hypoxia is a cause or a consequence of obesity-related metabolic disease.

VEGF is the key regulator of angiogenesis (Carmeliet, 2003; Folkman, 1995). In a variety of tissues, changes in VEGF activity positively correlate with microvascular density and hence blood perfusion, which governs the oxygenation of tissues (Baffert et al., 2006; Kamba et al., 2006). In adipose tissue, VEGF expression is differentially regulated depending on the anatomical locations of the fat depot and dysregulated in obese individuals (Cao, 2007; Goossens et al., 2011; Halberg et al., 2009; Liu et al., 2010; Miyazawa-Hoshimoto et al., 2005; Pasarica et al., 2009). To alter tissue perfusion via modulation of adipose blood vessel density, we employed genetically engineered mouse models to generate VEGF deficiency (i.e., loss of function, LOF) or doxycycline-inducible overexpression (i.e., gain of function, GOF) restricted to the adipose tissue. In both cases, the well-characterized aP2-Cre transgenic mice (He et al., 2003) provided the desired specificity. The aP2 promoter is active in white and brown adipocytes as well as macrophages (Fu et al., 2000; Furuhashi et al., 2008; Makowski et al., 2001), rendering it ideally suited to generate adipose-specific VEGF alterations. Although the adipose specificity of the aP2-Cre transgene is well characterized, there are reports indicating that a HFD could induce ectopic aP2 expression in other metabolically important organs (Segal et al., 1992). Therefore, we evaluated the expression of Fabp4 (aP2) and VEGF levels in the liver and muscles. We did not detect any changes in these tissues (Figure S2D), which ruled out the possibility that other organs played direct VEGF level-dependent roles in the development of the VEGF$^{Ad\Delta}$ and VEGF^{AdTg} phenotypes.

Young animals challenged with a HFD developed severe hypoxia, adipocyte apoptosis, and inflammation, which eventually led to insulin resistance. The associated lipid accumulation in

insulin-sensitive organs further suggested that the vascular network in adipose tissue is a critical determinant for adipose lipid storage capacity. When the low vessel density-determined storage capacity of the adipose tissue was surpassed, lipid was deposited into ectopic sites including brown fat, liver, and muscle. The ectopic fat is likely to cause lipotoxicity in the liver and muscles, contributing to the development of insulin resistance (Kim et al., 2007; Savage, 2009; Virtue and Vidal-Puig, 2010). We showed that the VEGF-induced vessel density increase in the adipose led to the reversal of metabolic morbidities caused by HFD. In these mice, decreased levels of hypoxia and fat inflammation and reduction of adipocyte size were accompanied by the restoration of normal adipose function.

A number of recent publications have investigated the role of VEGF in physiological processes including adipose function (Elias et al., 2012; Lu et al., 2012; Sun et al., 2012). In addition, another member of VEGF family, VEGF-B, has also been shown to regulate lipid transportation and insulin resistance (Hagberg et al., 2010, 2012). These studies, along with our data, highlight the unexpected roles of angiogenic growth factors in whole-body metabolism and unveiled their therapeutic potential for the treatment of metabolic disease and diabetes (Carmeliet et al., 2012).

In light of both our LOF and GOF findings, it is intriguing and seemingly contradictory that a number of preclinical studies have shown metabolic improvement after treatment with anti-angiogenic agents (Gregor and Hotamisligil, 2007; Houstis et al., 2006; Sun et al., 2012). We believe that a significant part of this discrepancy arises from the systemic nature of inhibition modalities, which could affect metabolically important nonadipose tissues such as liver, skeletal muscle, and heart as well as energy expenditure and the hypothalamic appetite control (Bråkenhielm et al., 2004; Gaemers et al., 2011; Liu et al., 2010; Virtue and Vidal-Puig, 2010). These systemic effects (Lu et al., 2012) may create unknown influences on whole-body metabolism either directly or indirectly by stimulating other angiogenic growth factors such as VEGF-B, which regulate transendothelial fatty acid transportation in metabolically active organs (Hagberg et al., 2010, 2012). These notions further emphasize the necessity of models with adipose-specific VEGF deficiency, like the one reported here.

Another reason could be the fact that systemic antiangiogenic therapies were applied on animals that were already obese (Houstis et al., 2006; Ozcan et al., 2004; Sun et al., 2012). In our LOF study, however, angiogenesis was reduced in normal adipose tissue. It is possible that in obese individuals, the anti-angiogenic treatment of severely hypoxic adipose tissues ablates a large proportion of the failing adipocytes, which gives space for a healthier, less hypoxic regeneration of the adipose tissue.

Regarding our GOF studies, metabolic protection by increased adipose VEGF expression (started prior to HFD feeding) has been already demonstrated (Elias et al., 2012; Sun et al., 2012). Here we stepped further and asked if adipose VEGF activation (started at the time, when HFD already established metabolic anomaly) could reverse the disease. We found that the increased blood vessel density achieved by VEGF induction in deteriorating fat improves adipose function by increasing blood perfusion, decreasing adipocyte size, reducing hypoxia, and thereby preventing adipocyte apoptosis or necrosis. These findings led to the important notion that obese adipose failure is reversible, mediated by sufficient vessel density determined by VEGF expression. Adipose-VEGF induction reverts the consequence of a cascade of events: adipose hypoxia, adipocyte apoptosis, adipose inflammation, ectopic lipid deposition, and lipotoxicity in metabolically compromised animals, and restores normal glucose homeostasis.

The possibility of adipose-specific modulation of VEGF signaling opens up novel therapeutic avenues to treat type 2 diabetes and the current epidemic of obesity-related metabolic diseases.

EXPERIMENTAL PROCEDURES

Animal Maintenance and Studies

All animal care and experimental procedures were approved by the Animal Care Committees of the Toronto Centre for Phenogenomic (TCP). The colony was housed in a specific pathogen-free (SPF) facility in ventilated cages with controlled environment settings (70°F–72°F, 30%–60% humidity), 12 hr light and dark cycles, and ad libitum access to water and food (see the Supplemental Information for more information).

Histologic and Morphometric Analysis

Mouse tissues were prefixed by perfusion with 1% paraformaldehyde in PBS. WATs were harvested and used as whole mount, while other tissues, including liver and brown adipose tissue after postfixation with 4% paraformaldehyde, were embedded in paraffin for sections and hematoxylin and eosin staining (see the Supplemental Information for more information).

Statistical Analyses

All calculations were performed using PRISM 5.0C software (GraphPad, San Diego, CA, USA) and Microsoft Excel 2011 for Mac. Statistical significance between two groups was determined by the Student's t test using Microsoft Excel and PRISM 5.0C. All data are presented as mean ± SEM.

SUPPLEMENTAL INFORMATION

Supplemental Information includes seven figures, Supplemental Experimental Procedures, and one table and can be found with this article at http://dx.doi.org/10.1016/j.cmet.2012.12.010.

ACKNOWLEDGMENTS

We would like to thank Drs. Patrick Tam and Daniel J. Drucker for critical reading of the manuscript. We also thank Dawei Qu, Ken Harpal, John Hsien, and Ariana Karanxha for their excellent technical support. We are grateful to Drs. So-Young Park, Yong Woon Kim, and Jae Ryong Kim at Yeungnam University, Korea, for the critical discussion and intellectual input. We would like to thank the staff of the Toronto Centre for Phenogenomics (TCP), especially Michael Copada, for excellent technical support. H.-K.S. was a recipient of the Gail Posluns Fellowship in Haematology (2007–2009). J.G.P. was a recipient of a Canadian Institutes of Health Research Fellowship (2006–2009). This work was supported by a grant to A.N. from NCIC-Terry Fox Foundation (105268), supported in part by a National Research Foundation of Korea (NRF) grant to Medical Research Center at Yeungnam University (K.-O.D.), and funded by the Korea government (MEST) (2011-0006185) and by a Premier's Summit Award to T.P.

Received: September 22, 2011
Revised: October 11, 2012
Accepted: December 17, 2012
Published: January 8, 2013

REFERENCES

Akeson, A.L., Greenberg, J.M., Cameron, J.E., Thompson, F.Y., Brooks, S.K., Wiginton, D., and Whitsett, J.A. (2003). Temporal and spatial regulation of VEGF-A controls vascular patterning in the embryonic lung. Dev. Biol. *264*, 443–455.

Baffert, F., Le, T., Sennino, B., Thurston, G., Kuo, C.J., Hu-Lowe, D., and McDonald, D.M. (2006). Cellular changes in normal blood capillaries undergoing regression after inhibition of VEGF signaling. Am. J. Physiol. Heart Circ. Physiol. *290*, H547–H559.

Basaria, S., Braga, M., and Moore, W.T. (2002). Doxycycline-induced hypoglycemia in a nondiabetic young man. South. Med. J. *95*, 1353–1354.

Belteki, G., Haigh, J., Kabacs, N., Haigh, K., Sison, K., Costantini, F., Whitsett, J., Quaggin, S.E., and Nagy, A. (2005). Conditional and inducible transgene expression in mice through the combinatorial use of Cre-mediated recombination and tetracycline induction. Nucleic Acids Res. *33*, e51. http://dx.doi.org/10.1093/nar/gni051.

Bråkenhielm, E., Cao, R., Gao, B., Angelin, B., Cannon, B., Parini, P., and Cao, Y. (2004). Angiogenesis inhibitor, TNP-470, prevents diet-induced and genetic obesity in mice. Circ. Res. *94*, 1579–1588.

Cao, Y. (2007). Angiogenesis modulates adipogenesis and obesity. J. Clin. Invest. *117*, 2362–2368.

Cao, Y. (2010). Adipose tissue angiogenesis as a therapeutic target for obesity and metabolic diseases. Nat. Rev. Drug Discov. *9*, 107–115.

Carmeliet, P. (2003). Angiogenesis in health and disease. Nat. Med. *9*, 653–660.

Carmeliet, P., Wong, B.W., and De Bock, K. (2012). Treating diabetes by blocking a vascular growth factor. Cell Metab. *16*, 553–555.

Chi, J.T., Wang, Z., Nuyten, D.S., Rodriguez, E.H., Schaner, M.E., Salim, A., Wang, Y., Kristensen, G.B., Helland, A., Børresen-Dale, A.L., et al. (2006). Gene expression programs in response to hypoxia: cell type specificity and prognostic significance in human cancers. PLoS Med. *3*, e47. http://dx.doi.org/10.1371/journal.pmed.0030047.

Cho, C.H., Koh, Y.J., Han, J., Sung, H.K., Jong Lee, H., Morisada, T., Schwendener, R.A., Brekken, R.A., Kang, G., Oike, Y., et al. (2007). Angiogenic role of LYVE-1-positive macrophages in adipose tissue. Circ. Res. *100*, e47–e57.

Christiaens, V., and Lijnen, H.R. (2010). Angiogenesis and development of adipose tissue. Mol. Cell. Endocrinol. *318*, 2–9.

Cinti, S., Mitchell, G., Barbatelli, G., Murano, I., Ceresi, E., Faloia, E., Wang, S., Fortier, M., Greenberg, A.S., and Obin, M.S. (2005). Adipocyte death defines macrophage localization and function in adipose tissue of obese mice and humans. J. Lipid Res. *46*, 2347–2355.

Elias, I., Franckhauser, S., Ferré, T., Vilà, L., Tafuro, S., Muñoz, S., Roca, C., Ramos, D., Pujol, A., Riu, E., et al. (2012). Adipose tissue overexpression of vascular endothelial growth factor protects against diet-induced obesity and insulin resistance. Diabetes *61*, 1801–1813.

Ema, M., Takahashi, S., and Rossant, J. (2006). Deletion of the selection cassette, but not cis-acting elements, in targeted Flk1-lacZ allele reveals Flk1 expression in multipotent mesodermal progenitors. Blood *107*, 111–117.

Folkman, J. (1995). Angiogenesis in cancer, vascular, rheumatoid and other disease. Nat. Med. *1*, 27–31.

Fong, G.H., Rossant, J., Gertsenstein, M., and Breitman, M.L. (1995). Role of the Flt-1 receptor tyrosine kinase in regulating the assembly of vascular endothelium. Nature *376*, 66–70.

Fu, Y., Luo, N., and Lopes-Virella, M.F. (2000). Oxidized LDL induces the expression of ALBP/aP2 mRNA and protein in human THP-1 macrophages. J. Lipid Res. *41*, 2017–2023.

Furuhashi, M., Fucho, R., Görgün, C.Z., Tuncman, G., Cao, H., and Hotamisligil, G.S. (2008). Adipocyte/macrophage fatty acid-binding proteins contribute to metabolic deterioration through actions in both macrophages and adipocytes in mice. J. Clin. Invest. *118*, 2640–2650.

Gaemers, I.C., Stallen, J.M., Kunne, C., Wallner, C., van Werven, J., Nederveen, A., and Lamers, W.H. (2011). Lipotoxicity and steatohepatitis in an overfed mouse model for non-alcoholic fatty liver disease. Biochim. Biophys. Acta *1812*, 447–458.

Garbitelli, V.P. (1987). Tetracycline reduces the need for insulin. N. Y. State J. Med. *87*, 576.

Gerber, H.P., Hillan, K.J., Ryan, A.M., Kowalski, J., Keller, G.A., Rangell, L., Wright, B.D., Radtke, F., Aguet, M., and Ferrara, N. (1999). VEGF is required for growth and survival in neonatal mice. Development *126*, 1149–1159.

Goossens, G.H., Bizzarri, A., Venteclef, N., Essers, Y., Cleutjens, J.P., Konings, E., Jocken, J.W., Cajlakovic, M., Ribitsch, V., Clément, K., and Blaak, E.E. (2011). Increased adipose tissue oxygen tension in obese compared with lean men is accompanied by insulin resistance, impaired adipose tissue capillarization, and inflammation. Circulation *124*, 67–76.

Gregor, M.F., and Hotamisligil, G.S. (2007). Thematic review series: Adipocyte Biology. Adipocyte stress: the endoplasmic reticulum and metabolic disease. J. Lipid Res. *48*, 1905–1914.

Hagberg, C.E., Falkevall, A., Wang, X., Larsson, E., Huusko, J., Nilsson, I., van Meeteren, L.A., Samen, E., Lu, L., Vanwildemeersch, M., et al. (2010). Vascular endothelial growth factor B controls endothelial fatty acid uptake. Nature *464*, 917–921.

Hagberg, C.E., Mehlem, A., Falkevall, A., Muhl, L., Fam, B.C., Ortsäter, H., Scotney, P., Nyqvist, D., Samén, E., Lu, L., et al. (2012). Targeting VEGF-B as a novel treatment for insulin resistance and type 2 diabetes. Nature *490*, 426–430.

Halberg, N., Khan, T., Trujillo, M.E., Wernstedt-Asterholm, I., Attie, A.D., Sherwani, S., Wang, Z.V., Landskroner-Eiger, S., Dineen, S., Magalang, U.J., et al. (2009). Hypoxia-inducible factor 1alpha induces fibrosis and insulin resistance in white adipose tissue. Mol. Cell. Biol. *29*, 4467–4483.

Hausman, G.J., and Richardson, R.L. (2004). Adipose tissue angiogenesis. J. Anim. Sci. *82*, 925–934.

He, W., Barak, Y., Hevener, A., Olson, P., Liao, D., Le, J., Nelson, M., Ong, E., Olefsky, J.M., and Evans, R.M. (2003). Adipose-specific peroxisome proliferator-activated receptor gamma knockout causes insulin resistance in fat and liver but not in muscle. Proc. Natl. Acad. Sci. USA *100*, 15712–15717.

Hosogai, N., Fukuhara, A., Oshima, K., Miyata, Y., Tanaka, S., Segawa, K., Furukawa, S., Tochino, Y., Komuro, R., Matsuda, M., and Shimomura, I. (2007). Adipose tissue hypoxia in obesity and its impact on adipocytokine dysregulation. Diabetes *56*, 901–911.

Hotamisligil, G.S. (2006). Inflammation and metabolic disorders. Nature *444*, 860–867.

Houstis, N., Rosen, E.D., and Lander, E.S. (2006). Reactive oxygen species have a causal role in multiple forms of insulin resistance. Nature *440*, 944–948.

Kamba, T., Tam, B.Y., Hashizume, H., Haskell, A., Sennino, B., Mancuso, M.R., Norberg, S.M., O'Brien, S.M., Davis, R.B., Gowen, L.C., et al. (2006). VEGF-dependent plasticity of fenestrated capillaries in the normal adult microvasculature. Am. J. Physiol. Heart Circ. Physiol. *290*, H560–H576.

Kerbel, R.S. (2008). Tumor angiogenesis. N. Engl. J. Med. *358*, 2039–2049.

Kim, J.Y., van de Wall, E., Laplante, M., Azzara, A., Trujillo, M.E., Hofmann, S.M., Schraw, T., Durand, J.L., Li, H., Li, G., et al. (2007). Obesity-associated improvements in metabolic profile through expansion of adipose tissue. J. Clin. Invest. *117*, 2621–2637.

Lijnen, H.R. (2008). Angiogenesis and obesity. Cardiovasc. Res. *78*, 286–293.

Lijnen, H.R., Christiaens, V., Scroyen, I., Voros, G., Tjwa, M., Carmeliet, P., and Collen, D. (2006). Impaired adipose tissue development in mice with inactivation of placental growth factor function. Diabetes *55*, 2698–2704.

Liu, X., Hao, L., Zhang, S., Ji, Y., Zhang, Y., Lu, X., Shi, B., Pei, H., Wang, Y., Chen, D., et al. (2010). Genetic repression of mouse VEGF expression regulates coagulation cascade. IUBMB Life *62*, 819–824.

Lu, X., Ji, Y., Zhang, L., Zhang, Y., Zhang, S., An, Y., Liu, P., and Zheng, Y. (2012). Resistance to obesity by repression of VEGF gene expression through induction of brown-like adipocyte differentiation. Endocrinology *153*, 3123–3132.

Makowski, L., Boord, J.B., Maeda, K., Babaev, V.R., Uysal, K.T., Morgan, M.A., Parker, R.A., Suttles, J., Fazio, S., Hotamisligil, G.S., and Linton, M.F.

(2001). Lack of macrophage fatty-acid-binding protein aP2 protects mice deficient in apolipoprotein E against atherosclerosis. Nat. Med. *7*, 699–705.

Mick, G.J., Wang, X., and McCormick, K. (2002). White adipocyte vascular endothelial growth factor: regulation by insulin. Endocrinology *143*, 948–953.

Miyazawa-Hoshimoto, S., Takahashi, K., Bujo, H., Hashimoto, N., and Saito, Y. (2003). Elevated serum vascular endothelial growth factor is associated with visceral fat accumulation in human obese subjects. Diabetologia *46*, 1483–1488.

Miyazawa-Hoshimoto, S., Takahashi, K., Bujo, H., Hashimoto, N., Yagui, K., and Saito, Y. (2005). Roles of degree of fat deposition and its localization on VEGF expression in adipocytes. Am. J. Physiol. Endocrinol. Metab. *288*, E1128–E1136.

Odeh, M., and Oliven, A. (2000). Doxycycline-induced hypoglycemia. J. Clin. Pharmacol. *40*, 1173–1174.

Ozawa, C.R., Banfi, A., Glazer, N.L., Thurston, G., Springer, M.L., Kraft, P.E., McDonald, D.M., and Blau, H.M. (2004). Microenvironmental VEGF concentration, not total dose, determines a threshold between normal and aberrant angiogenesis. J. Clin. Invest. *113*, 516–527.

Ozcan, U., Cao, Q., Yilmaz, E., Lee, A.H., Iwakoshi, N.N., Ozdelen, E., Tuncman, G., Görgün, C., Glimcher, L.H., and Hotamisligil, G.S. (2004). Endoplasmic reticulum stress links obesity, insulin action, and type 2 diabetes. Science *306*, 457–461.

Pasarica, M., Sereda, O.R., Redman, L.M., Albarado, D.C., Hymel, D.T., Roan, L.E., Rood, J.C., Burk, D.H., and Smith, S.R. (2009). Reduced adipose tissue oxygenation in human obesity: evidence for rarefaction, macrophage chemotaxis, and inflammation without an angiogenic response. Diabetes *58*, 718–725.

Pasarica, M., Rood, J., Ravussin, E., Schwarz, J.M., Smith, S.R., and Redman, L.M. (2010). Reduced oxygenation in human obese adipose tissue is associated with impaired insulin suppression of lipolysis. J. Clin. Endocrinol. Metab. *95*, 4052–4055.

Rupnick, M.A., Panigrahy, D., Zhang, C.Y., Dallabrida, S.M., Lowell, B.B., Langer, R., and Folkman, M.J. (2002). Adipose tissue mass can be regulated through the vasculature. Proc. Natl. Acad. Sci. USA *99*, 10730–10735.

Savage, D.B. (2009). Mouse models of inherited lipodystrophy. Dis. Model. Mech. *2*, 554–562.

Segal, K.R., Albu, J., Chun, A., Edano, A., Legaspi, B., and Pi-Sunyer, F.X. (1992). Independent effects of obesity and insulin resistance on postprandial thermogenesis in men. J. Clin. Invest. *89*, 824–833.

Strissel, K.J., Stancheva, Z., Miyoshi, H., Perfield, J.W., 2nd, DeFuria, J., Jick, Z., Greenberg, A.S., and Obin, M.S. (2007). Adipocyte death, adipose tissue remodeling, and obesity complications. Diabetes *56*, 2910–2918.

Sun, K., Wernstedt Asterholm, I., Kusminski, C.M., Bueno, A.C., Wang, Z.V., Pollard, J.W., Brekken, R.A., and Scherer, P.E. (2012). Dichotomous effects of VEGF-A on adipose tissue dysfunction. Proc. Natl. Acad. Sci. USA *109*, 5874–5879.

Trayhurn, P., Wang, B., and Wood, I.S. (2008). Hypoxia in adipose tissue: a basis for the dysregulation of tissue function in obesity? Br. J. Nutr. *100*, 227–235.

Virtue, S., and Vidal-Puig, A. (2010). Adipose tissue expandability, lipotoxicity and the Metabolic Syndrome—an allostatic perspective. Biochim. Biophys. Acta *1801*, 338–349.

Waki, H., and Tontonoz, P. (2007). Endocrine functions of adipose tissue. Annu. Rev. Pathol. *2*, 31–56.

Weisberg, S.P., McCann, D., Desai, M., Rosenbaum, M., Leibel, R.L., and Ferrante, A.W., Jr. (2003). Obesity is associated with macrophage accumulation in adipose tissue. J. Clin. Invest. *112*, 1796–1808.

Wellen, K.E., and Hotamisligil, G.S. (2005). Inflammation, stress, and diabetes. J. Clin. Invest. *115*, 1111–1119.

WHO (2010). 10 facts on obesity. WHO website, http://www.who.int/features/factfiles/obesity/en/.

Wood, I.S., de Heredia, F.P., Wang, B., and Trayhurn, P. (2009). Cellular hypoxia and adipose tissue dysfunction in obesity. Proc. Nutr. Soc. *68*, 370–377.

Xu, H., Barnes, G.T., Yang, Q., Tan, G., Yang, D., Chou, C.J., Sole, J., Nichols, A., Ross, J.S., Tartaglia, L.A., and Chen, H. (2003). Chronic inflammation in fat plays a crucial role in the development of obesity-related insulin resistance. J. Clin. Invest. *112*, 1821–1830.

Yach, D., Stuckler, D., and Brownell, K.D. (2006). Epidemiologic and economic consequences of the global epidemics of obesity and diabetes. Nat. Med. *12*, 62–66.

Yamauchi, T., Kamon, J., Waki, H., Terauchi, Y., Kubota, N., Hara, K., Mori, Y., Ide, T., Murakami, K., Tsuboyama-Kasaoka, N., et al. (2001). The fat-derived hormone adiponectin reverses insulin resistance associated with both lipoatrophy and obesity. Nat. Med. *7*, 941–946.

Yamauchi, T., Kamon, J., Minokoshi, Y., Ito, Y., Waki, H., Uchida, S., Yamashita, S., Noda, M., Kita, S., Ueki, K., et al. (2002). Adiponectin stimulates glucose utilization and fatty-acid oxidation by activating AMP-activated protein kinase. Nat. Med. *8*, 1288–1295.

Yin, J., Gao, Z., He, Q., Zhou, D., Guo, Z., and Ye, J. (2009). Role of hypoxia in obesity-induced disorders of glucose and lipid metabolism in adipose tissue. Am. J. Physiol. Endocrinol. Metab. *296*, E333–E342.

Zhang, Q.X., Magovern, C.J., Mack, C.A., Budenbender, K.T., Ko, W., and Rosengart, T.K. (1997). Vascular endothelial growth factor is the major angiogenic factor in omentum: mechanism of the omentum-mediated angiogenesis. J. Surg. Res. *67*, 147–154.